Short Papers

New Uniplanar Subnanosecond Monocycle Pulse Generator and Transformer for Time-Domain Microwave Applications

Jeong Soo Lee, Cam Nguyen, and Tom Scullion

***Abstract*—This paper presents the development of a new monocycle pulse generator and pulse-to-monocycle-pulse transformer operating in the subnanosecond regime. These circuits employ Schottky diodes, step recovery diodes, and simple charging and discharging circuitry, and are completely fabricated using coplanar waveguides. Simple transient analysis and design of the circuits are presented along with their operating principles. The pulse-to-monocycle-pulse transformer converts a 1-V 300-ps pulse into a 0.7-V 350-ps monocycle pulse. The monocycle pulse generator produces a monocycle pulse having 333-ps pulsewidth and more than 2 V from an input square wave of 10-MHz repetition rate. The generated monocycle pulses have very symmetrical positive and negative portions and low ringing level.**

***Index Terms*—MIC, pulse generator, transmitter, ultra-wide-band radar, uniplanar circuits.**

I. Introduction

Time-domain measurement systems, such as pulsed radar, are important in many scientific and engineering disciplines. One of the most important applications of these systems is perhaps subsurface sensing, which has recently attracted a widespread interest in various engineering fields. The pulse generator is an essential component for these systems. In general, a monocycle pulse generator is preferred over an impulse generator because it has a much narrower bandwidth. This considerably eases the design of other system components. Using the frozen-wave concept with a high-speed optically activated photoconductive switch, high amplitude and short pulses were attained with laser sources [1], [2]. Monocyle pulses have been generated using spark gaps [3]. Pulse generators can also be realized using transistors operating in the avalanche mode or step-recovery diodes (SRDs). The repetition rate of transistor pulse generators, however, cannot be larger than 10 MHz due to overheating, which is caused by the avalanching [4]. SRD is perhaps the most commonly used device for pulse generation. An SRD impulse generator using lumped elements was presented in [5]. An impulse generator, consisting of an SRD connected in shunt across a microstrip line, was also developed [6]. Novel nonlinear transmission lines (NLTLs) implemented with Schottky diodes connected in shunt across coplanar waveguides (CPWs) or microstrip lines have also been used to generate pulses [7], [8]. These NLTL pulse generators, however, are more suitable for monolithic microwave integrated circuits (MMICs) than hybrid microwave integrated circuits (HMICs) due to the use of many Schottky diodes periodically located along the transmission line. Moreover, the size of these circuits may be prohibitively large for practical commercial MMICs, even at lower millimeter-wave frequencies.

In this paper, we report the development of a new monocycle pulse generator and pulse-to-monocycle-pulse transformer utilizing an SRD, Schottky diode, and CPW. As will be seen later, we implement a novel concept of switching the transmission line automatically using charging and discharging circuits, and the circuits are completely different from those reported in literature. These circuits are fabricated using uniplanar transmission lines and, hence, are highly desirable because of ease in mounting solid-state devices, elimination of via holes, and requirement of only single-sided circuit processing, all leading to circuit simplicity and low cost. They are ideal for low-cost microwave applications, including MMICs and HMICs.

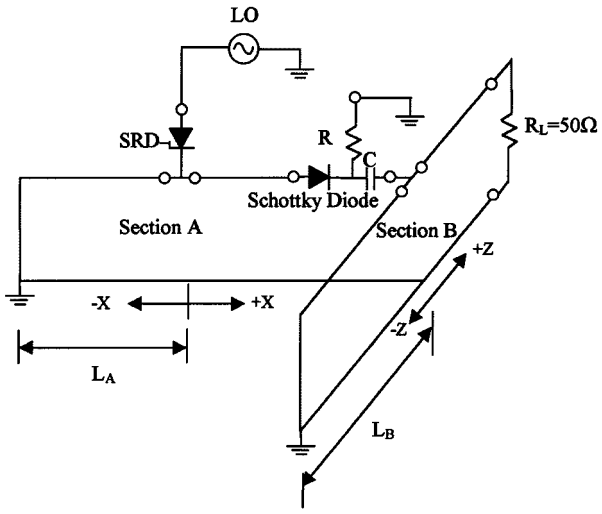

Fig. 1. Circuit diagram of the new monocycle pulse generator.

II. Operating Principle and Analysis

A. Operating Principle

Fig. 1 shows the circuit diagram of the new monocycle pulse generator. It is composed of an SRD, a Schottky diode, a capacitor (C), a resistor (R), and two 50-Ω short-circuited transmission lines (sections A and B). The local oscillator (LO) source of 10 MHz is external and used to supply a square-wave signal to the SRD, which generates a step-like pulse. This step pulse divides into two other step pulses upon arriving at the transmission line A, which then propagate to the $\pm x$-directions. The step pulse traveling toward the short circuit is reflected back and eventually combines with the other step pulse to form a Gaussian-like pulse. The pulsewidth t_g of this resultant pulse is given by the following expression:

$$t_g = \frac{2L_A}{u_p} \tag{1}$$

where u_p is the phase velocity along the transmission line A. The rising and falling transition time of the pulse depend on the SRD and, in general, they are in the range of 30–150 ps for practical SRDs. This

Manuscript received July 5, 2000. This work was supported in part by the Texas Department of Transportation, by the Interdisciplinary Research Program, by the Southwest Region University Transportation Center, and by the Texas Transportation Institute.

J. S. Lee was with the Sensing, Imaging, and Communications Systems Laboratory, Department of Electrical Engineering, Texas A&M University, College Station, TX 77843-3128 USA. He is now with Filtronic Solid State, Santa Clara, CA 95054 USA.

C. Nguyen is with the Sensing, Imaging, and Communications Systems Laboratory, Department of Electrical Engineering, Texas A&M University, College Station, TX 77843-3128 USA.

T. Scullion is with the Texas Transportation Institute, Texas A&M University, College Station, TX 77843-3128 USA.

Publisher Item Identifier S 0018-9480(01)03983-7.

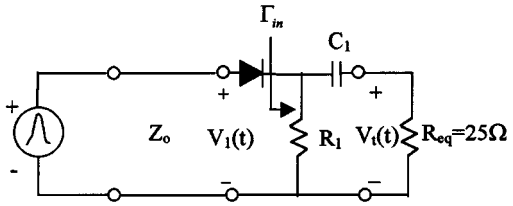

Fig. 2. Simplified transient equivalent circuit.

pulse then propagates toward the Schottky diode and, upon reaching the diode, its rising edge turns the diode on and charges the capacitor C. The pulse then passes through a high-pass filter, formed by the capacitor C and the resistor $R_{\rm eq}$ representing the $-$ and $+$ z-portions of section B under a transient condition (see Fig. 2), allowing only the leading- and trailing-edge parts of this incident wave to be transmitted through the junction at section B into the $\pm z$-directions. The pulse propagating in the $-z$-direction is reversed at the short circuit and propagates toward the load ($R_{\rm L}$); this negative pulse eventually arrives at the load and combines with the other positive pulse to form a monocycle pulse. As will be seen later, once the incident wave is transmitted across the junction, the stored charge in the capacitor C would provide a self reverse bias to the diode and effectively remove the loading of section A, Schottky diode, R, and C upon section B, thereby preventing them from disturbing the pulses propagating along section B. In addition to this blocking function of C, it also, together with the resistor R, provides a discharging loop for the next incoming pulse. To facilitate this discharging function, the time constant *RC* should be designed to be smaller than the desired pulse repetition rate.

B. Analysis and Design

Fig. 2 shows a simplified equivalent circuit, under a transient operation, seen by the pulse approaching the Schottky diode. Note that $R_{\rm eq}$ represents the combination of the $\pm z$-directed portions of section B at the junction under the transient condition. This simple transient equivalent circuit is used to approximately analyze the charging and transmitting process at the junction of section B, and help explain the operating principle of the monocycle pulse generator. Assuming the Schottky diode behaves as an ideal switch, we can write

$$R_{\rm eq}C\frac{dV_{\rm C}(t)}{dt}+V_{\rm C}(t)=V_{\rm i}(t) \tag{2}$$

where $V_{\rm i}(t)$ is the voltage of the pulse incident upon the diode, which is assumed to be a triangular function; $V_{\rm C}(t)$ represents the voltage drop across the capacitor C and is given by

$$V_{\rm C}(t)=A\left[\tau e^{-t/\tau}-\tau+t\right]U(t)-2A\times\left[\left(t-\frac{T}{2}\right)-\tau+\tau e^{-(t-T/2)/\tau}\right]U\left(t-\frac{T}{2}\right) \tag{3}$$

where $\tau=R_{\rm eq}C$ is the time constant, A is the positive slope of incident triangular pulse $V_{\rm i}(t)$, $U(t)$ is the unit step function, and T is the duration of the triangular pulse. The voltage of the pulse transmitted into section B can be found from

$$V_{\rm t}(t)=V_{\rm i}(t)-V_{\rm C}(t)-V_{\rm D} \tag{4}$$

where $V_{\rm D}$ denotes the voltage drop across the diode. These equations are only valid up to the time when $V_{\rm C}(t)$ is equal to $V_{\rm i}(t)$ since the diode begins to be reverse-biased afterward. $V_{\rm C}$ then remains almost constant until the next pulse arrives since there is no rapid discharging pass for the capacitor. Note that the diode is open even before the trailing edge of the incident triangular pulse reaches zero. Fig. 3 shows the calculated transient responses of the incident voltage, voltage across the capacitor, and voltage of the transmitted pulse.

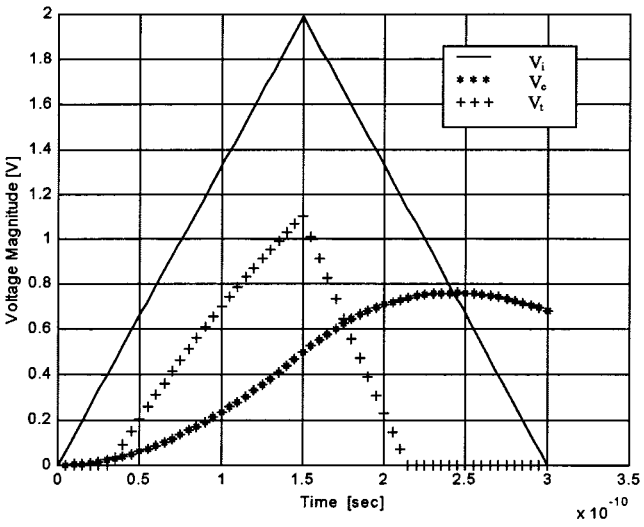

Fig. 3. Transient responses of $V_{\rm i}(t)$, $V_{\rm C}(t)$, and $V_{\rm t}(t)$.

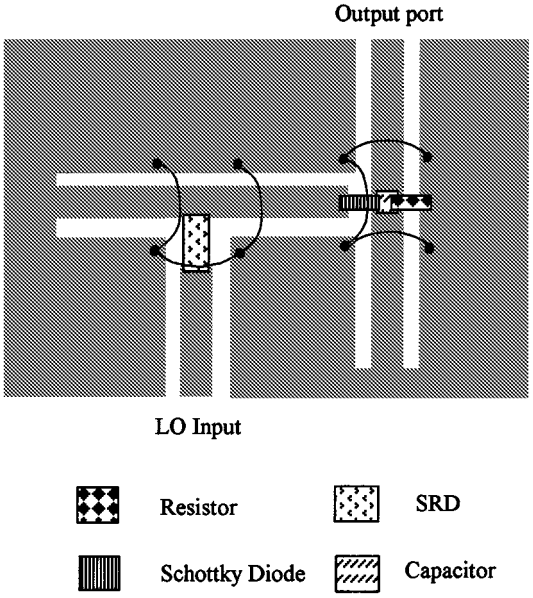

Fig. 4. Layout of the monocycle pulse generator.

As the pulse operates over an extremely wide bandwidth, the matching cannot be achieved completely whether the diode is on or off. The incoming pulse from section A is partly reflected back from the junction at section B; this reflected wave is bounced back and forth within section A, primarily causing the ringing of the final monocycle pulse propagating in section B. To reduce the multiple reflections in section A, shunt resistor can be used in section A with a slight sacrifice of the output voltage amplitude. The attenuation due to this extra resistor can also increase the pulse repetition rate.

III. Circuit Fabrication and Performance

Fig. 4 shows a layout of the monocycle pulse generator. The layout for the pulse-to-monocycle-pulse generator is the same, but without the SRD and short-circuited portion of section A. These circuits were fabricated using CPW on an RT/Duroid 6010 substrate with a relative dielectric constant of 10.2 and a thickness of 0.050 in. The Schottky

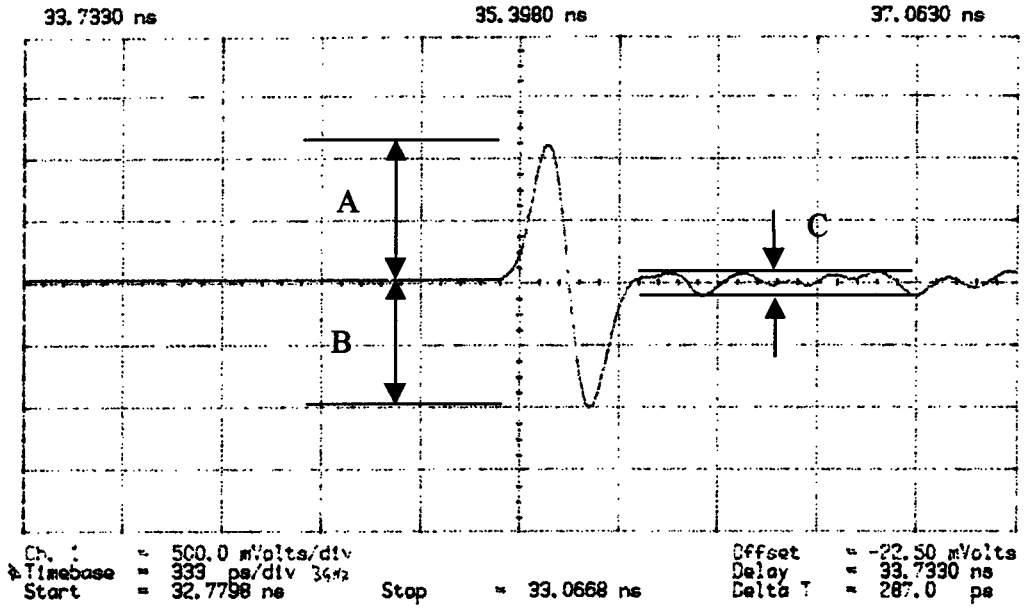

Fig. 5. Measured output pulse of the monocycle pulse generator.

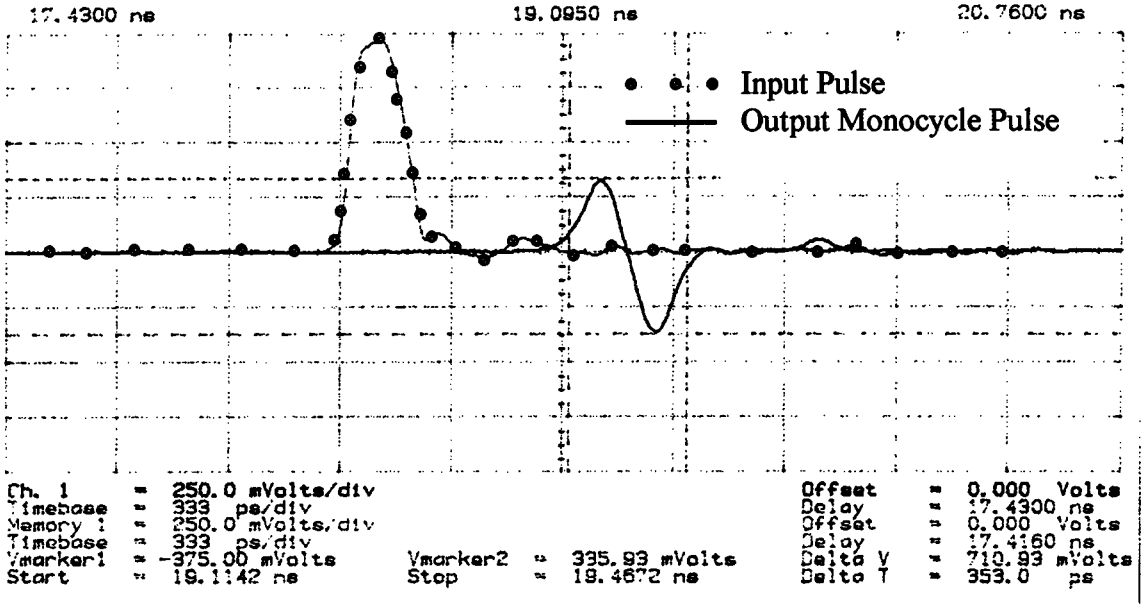

Fig. 6. Measured output pulse of the pulse-to-monocycle-pulse transformer.

diode used is a Hewlett-Packard HSCH-5336 beam-lead diode having junction and package capacitances of around 0.25 and 0.02 pF, respectively. The SRD is MMD-0840, which has a 10-ns nominal lifetime, 75-ps transition time, and 0.6-pF junction capacitance. A 5-pF chip capacitor (C) and 1-kΩ chip resistor (R) were used for charging and discharging, respectively.

For the monocycle pulse generator, we used an oscillator, generating a square wave with 10-ns risetime at 10 MHz, as the input LO source. Fig. 5 shows the signal measured at the output port of the generator. As can be seen, a monocycle pulse with more than 2 V_{p-p} (peak-to-peak) and 333-ps pulsewidth is obtained. The positive and negative parts of the pulse is also well balanced ($B/A > 93\%$), and the ringing level is relatively small ($C/(A+B) < 9\%$), even no tuning was made.

A 4050RPH pulse generator and PSPL-10050 pulse driver, from Picosecond Pulse Laboratories, Boulder, CO, were used to drive the pulse-to-monocycle-pulse transformer. Fig. 6 shows the measured output monocycle pulse superimposed with the input pulse. For an input pulse of 1 V and 300-ps pulsewidth, a monocycle pulse of 0.7 V_{pp} and 350-ps pulsewidth is obtained. The balance between the positive and negative parts of the monocycle pulse and its ringing level are similar to those obtained in the monocycle pulse generator.

IV. Conclusion

In this paper, we reported on the development of a new uniplanar monocycle pulse generator and pulse-to-monocycle-pulse transformer. Simple and approximate transient analysis of the transient behavior has been derived for the monocycle-pulse generator and helped explain the circuit operating principle. The pulse-to-monocycle-pulse transformer converts a 1-V 300-ps pulse into a 0.7-V 350-ps monocycle pulse, and the monocycle pulse generator generates a monocycle pulse having 333-ps pulsewidth and more than 2 V from an input square wave

of 10-MHz repetition rate. Low ringing levels and high balances between the positive and negative parts of the monocycle pulses have also been achieved without any circuit tuning. The developed circuits are simple and completely uniplanar and, hence, are attractive for compact low-cost time-domain microwave systems such as subsurface sensing radar.

ACKNOWLEDGMENT

The authors wish to thank the anonymous reviewers for their useful comments and suggestions.

REFERENCES

[1] C. William, "High-power microwave generation using optically activated semiconductor switches," *IEEE Trans. Electron Devices*, vol. 37, pp. 2439–2448, Dec. 1990.
[2] C. H. Lee, "Picosecond optics and microwave technology," *IEEE Trans. Microwave Theory Tech.*, vol. 38, pp. 596–607, May 1990.
[3] V. G. Shpak *et al.*, "Active former of monocycle high-voltage subnanosecond pulses," in *12th IEEE Pulsed Power Conf. Dig.*, June 1999, pp. 1456–1459.
[4] J. Millman and H. Taub, *Pulse, Digital, and Switching Waveforms*. New York: McGraw-Hill, 1965, ch. 13, 20.
[5] J. L. Moll *et al.*, "Physical modeling of the step recovery diode for pulse and harmonic generation circuits," *Proc. IEEE*, vol. 57, pp. 1250–1259, July 1969.
[6] K. Madani *et al.*, "A 20-GHz microwave sampler," *IEEE Trans. Microwave Theory Tech.*, vol. 40, pp. 1960–1963, Oct. 1992.
[7] M. J. W. Rodwell *et al.*, "GaAs nonlinear transmission lines for picosecond pulse generation and millimeter-wave sampling," *IEEE Trans. Microwave Theory Tech.*, vol. 39, pp. 1194–1204, July 1991.
[8] D. Salameh and D. Linton, "Microstrip GaAs nonlinear transmission-line (NLTL) harmonic and pulse generators," *IEEE Trans. Microwave Theory Tech.*, vol. 47, pp. 1118–1121, July 1999.

An Inverse Technique to Evaluate Permittivity of Material in a Cavity

Kailash P. Thakur and Wayne S Holmes

***Abstract*—A numerical technique to estimate the dielectric constant and loss factor of a homogeneous dielectric material placed in an arbitrary shaped cavity has been developed. The values of S-parameters are measured experimentally by placing the sample in the cavity. Starting with a trial set of permittivity values, the computation is carried out using the finite-element method (FEM) to match the S-parameters around the fundamental resonance frequency. The FEM routine is run several times while optimizing the values of dielectric constant and conductivity of the sample. During the process of optimization, eight different measures of error between computed and experimental values of complex S-parameters are examined. It is found that there is no single measure of error, which can be minimized to estimate two parameters (dielectric constant and the loss factor), but the combination of errors has to be minimized to get the exact solution. The computer program can generate the solution with an accuracy of less than 0.01% in a few hours on a pentium-based personal computer.**

***Index Terms*—Cavity resonance, dielectric constant, FEM, inverse problem, Monte Carlo simulation.**

I. INTRODUCTION

The measurement of the dielectric constant and loss factor of a material plays an important role in microwave technology. There are several techniques developed for an accurate measurement of permittivity of the material [1]–[7]. The measurement technique at microwave frequencies can be classified in three groups: 1) by using some probe or microwave sensor; 2) by using a waveguide cell filled with the sample of dielectric, where there is restriction upon the sample size and its alignment in the waveguide cell; and 3) by using the cavity resonance.

In the third group of techniques, the shift in the resonance peak and Q values of the cavity with and without the sample generate the values of dielectric constant and loss factor of the sample using the perturbation method. However, there are limitations for the use of the perturbation method. The sample size should be very small compared to the dimension of the cavity so that the electric field inside the cavity does not change much due to the presence of the sample. In a large number of applications it is not always possible to have a sample of acceptable dimensions. For example, if we intend to measure the dielectric constant of an apple, it will not be a good idea to use the perturbation technique.

This paper presents the development of a numerical simulation technique to obtain the complex permittivity (dielectric constant and loss factor) of a dielectric material of an arbitrary shape placed in an arbitrary-shaped cavity by using the finite-element method (FEM). The experimental values of S-parameters around the fundamental resonance frequency are matched with the simulated data.

II. PROCEDURE

In principle, the geometry of the cavity and dimensions of the sample within the cavity has no restriction as long as the entire volume can be divided into discrete elements acceptable by the FEM routine. However, a simple rectangular geometry has been considered here for the

Manuscript received July 11, 2000. This work was supported by the New Zealand Foundation for Research Science and Technology under Contract C08806, Objective 4.

The authors are with the Imaging and Sensing Team, Industrial Research Ltd., Auckland, New Zealand (e-mail: k.thakur@irl.cri.nz).

Publisher Item Identifier S 0018-9480(01)03984-9.